| Journal Code: | Article ID | Dispatch: 06.08.11 | CE: Kristian Arniebel E. Dumalag |
|---|---|---|---|
| F L D | 2 6 6 9 | No. of Pages: 19 | ME: |

INTERNATIONAL JOURNAL FOR NUMERICAL METHODS IN FLUIDS
*Int. J. Numer. Meth. Fluids* (2011)
Published online in Wiley Online Library (wileyonlinelibrary.com). DOI: 10.1002/fld.2669

# A finite element formulation satisfying the discrete geometric conservation law based on averaged Jacobians

Mario A. Storti*,†, Luciano Garelli and Rodrigo R. Paz

*Centro Internacional de Métodos Computacionales en Ingeniería (CIMEC), INTEC-CONICET-UNL, Güemes 3450, (S3000GLN) Santa Fe, Argentina*



## SUMMARY

In this article, a new methodology for developing discrete geometric conservation law (DGCL) compliant formulations is presented. It is carried out in the context of the finite element method for general advective–diffusive systems on moving domains using an ALE scheme. There is an extensive literature about the impact of DGCL compliance on the stability and precision of time integration methods. In those articles, it has been proved that satisfying the DGCL is a necessary and sufficient condition for any ALE scheme to maintain on moving grids the nonlinear stability properties of its fixed-grid counterpart. However, only a few works proposed a methodology for obtaining a compliant scheme. In this work, a DGCL compliant scheme based on an averaged ALE Jacobians formulation is obtained. This new formulation is applied to the $\theta$ family of time integration methods. In addition, an extension to the three-point backward difference formula is given. With the aim to validate the averaged ALE Jacobians formulation, a set of numerical tests are performed. These tests include 2D and 3D diffusion problems with different mesh movements and the 2D compressible Navier–Stokes equations. Copyright © 2011 John Wiley & Sons, Ltd.

Received 4 October 2010; Revised 30 June 2011; Accepted 16 July 2011

KEY WORDS: geometric conservation law; ALE formulation; moving meshes; finite element method

## 1. INTRODUCTION

When dealing with partial differential equations that need to be solved on moving domains, like problems in the fluid–structure interaction area [1–4], one of the most used technique is the so-called ALE. The idea behind the ALE formulation is the introduction of a computational mesh, which moves with a velocity independent of the speed of the material particles. The ALE method was first proposed in the context of finite differences [5, 6], then it was extended to finite elements [7–9] and to finite volumes [10].

When an ALE formulation is used, the governing equations must be written in a moving domain, and additional terms related to the mesh velocity and position are introduced. The reformulated equations must be integrated in time. The common way to proceed is to use a classical time advancing scheme like the $\theta$ family [8, 11] or the backward differentiation formulas (BDFs) family. In this context, the DGCL may arise, and it is directly related to the evolution of the mesh velocity and the elements volume change. This law was introduced by Thomas and Lombard [12], and it is a consistency criterion in which the numerical method must be able to reproduce exactly a constant solution on a moving domain.

As noted by Étienne *et al.* [13], the effect of the DGCL on the stability of ALE schemes is still unclear and somewhat contradictory. In the work by Guillard and Farhat [14], it has been observed

*Correspondence to: Mario A. Storti, Centro Internacional de Métodos Computacionales en Ingeniería (CIMEC), INTEC-CONICET-UNL, Güemes 3450, (S3000GLN) Santa Fe, Argentina.

†E-mail: mario.storti@gmail.com

that the movement of the domain can degrade the accuracy and stability of the numerical scheme with respect to their counterpart on fixed domains. In this direction, many researchers have been working with the aim of linking the accuracy and the stability of numerical schemes on an ALE framework with the discrete version of the geometric conservation law [13–16]. In the article by Geuzaine *et al.* [17], it has been shown that satisfying the DGCL is neither a necessary nor a sufficient condition for an ALE scheme to preserve on moving grids its time accuracy established on fixed grids. In the work presented by Farhat *et al.* [18], it was proved that for nonlinear scalar problems, the DGCL requirement is a necessary and a sufficient condition for an ALE time integrator to preserve the nonlinear stability properties of its fixed-grid counterpart. Meanwhile, Boffi and Gastaldi [15] and Formaggia and Nobile [16] have shown that it is neither a necessary nor a sufficient condition for stability, except for the backward Euler scheme. Although the impact of the DGCL on the stability and precision of the time integration methods is controversial, there is a general consensus in the development of schemes that satisfy the DGCL, in particular for fluid–structure interaction problems [19–21, 23].

A straightforward way to satisfy the DGCL is to use a time integration rule with degree of precision $n_d \cdot s - 1$, where $n_d$ is the spatial dimension and $s$ is the order of the polynomial used to represent the time evolution of the nodal displacement within each time step. For example, in 3D problems with a linear in time reconstruction, a rule with degree of precision 2 should be used. Alternatively, the methodology proposed by Farhat and Geuzaine [22] to obtain an ALE extension for a given time integrator in fixed meshes could be used.

In this work, a new methodology, which is based on averaged ALE Jacobians is proposed to obtain DGCL compliant FEM formulations. It is applied to the $\theta$ family of time integration methods in general nonlinear advective–diffusive problems. In addition, an extension to the three-point BDF is given.

In a previous work [22], averaged coefficients are obtained by starting with a general integration scheme with a series of unknown parameters, which are then adjusted to preserve DGCL compliance and the temporal accuracy of the fixed mesh counterpart. In contrast, in this work, the geometric coefficients are obtained by averaging them over the time step so that precision is preserved and the DGCL is satisfied in a natural way.

Finally, to validate the averaged Jacobians formulation (AJF), a set of numerical tests are performed. This includes 2D/3D diffusion problems on moving meshes and 2D compressible Navier–Stokes equations.

## 2. VARIATIONAL FORMULATION FOR ADVECTIVE–DIFFUSIVE SYSTEM FOR MOVING MESHES USING ALE

Let us start with the derivation of the ALE formulation for a general advective–diffusive system [7, 8, 20]. The governing equation to be expressed in an ALE framework is

$$\frac{\partial U_j}{\partial t} + \left(\mathcal{F}^c_{jk}(\mathbf{U}) - \mathcal{F}^d_{jk}(\mathbf{U}, \nabla\mathbf{U})\right)_{,k} = 0, \text{ in } \Omega^t \tag{1}$$

where $1 \leqslant k \leqslant n_d$, $n_d$ is the number of spatial dimensions, $1 \leqslant j \leqslant m$, $m$ is the dimension of the state vector (e.g., $m = n_d + 2$ for compressible flow), $t$ is time, $(\,)_{,j}$ denotes derivative with respect to the $j$th spatial dimension, $\mathbf{U} \in \mathrm{IR}^n$ is the state vector, and $\mathcal{F}^{c,d}_{jk} \in \mathrm{IR}^{n\times n_d}$ are the convective and diffusive fluxes, respectively. Appropriate Dirichlet and Neumann conditions are imposed at the boundary.

As the problem is posed in a time-dependent domain $\Omega^t$, it can not be solved with standard fixed-domain methods so that it is assumed that there is an inversible and continuously differentiable map $\mathrm{x} = \boldsymbol{\chi}(\boldsymbol{\xi}, t)$ between the current domain $\Omega^t$ and a reference domain $\Omega^\xi$, which can be for instance the initial domain $\Omega^\xi = \Omega^{t=0}$, and $\boldsymbol{\xi}$ is the coordinate in the reference domain. The Jacobian of the transformation is

$$J = \left|\frac{\partial x_j}{\partial \xi_k}\right|, \tag{2}$$





DOI: 10.1002/fld

and satisfies the following volume balance equation

$$\left.\frac{\partial J}{\partial t}\right|_{\boldsymbol{\xi}} = J\,\frac{\partial \upsilon_k^*}{\partial x_k}, \tag{3}$$

where

$$\upsilon_k^* = \left.\frac{\partial x_k}{\partial t}\right|_{\boldsymbol{\xi}}, \tag{4}$$

are the components of the mesh velocity.

The variational formulation of Equation (1) is obtained multiplying with a weighting function $w(\mathbf{x},t) = w(\boldsymbol{\chi}(\mathrm{x},t))$ and integrating over the current domain $\Omega^t$

$$\int_{\Omega^t} w\,\frac{\partial U_j}{\partial t}\mathrm{d}\Omega^t + \int_{\Omega^t}\left[\mathcal{F}_{jk}^c - \mathcal{F}_{jk}^d\right]_{,k} w\,\mathrm{d}\Omega^t = 0. \tag{5}$$

The integrals are brought to the reference domain $\Omega^\xi$

$$\int_{\Omega^\xi} w\,\frac{\partial U_{Pj}}{\partial t} J\,\mathrm{d}\Omega^\xi + \int_{\Omega^\xi}\left[\mathcal{F}_{jk}^c - \mathcal{F}_{jk}^d\right]_{,k} wJ\,\mathrm{d}\Omega^\xi = 0, \tag{6}$$

and the temporal derivative term can be converted to the reference mesh by noting that the partial derivative of $U_j$ is in fact a partial derivative at $\mathrm{x} =$ constant and then can be converted to a partial derivative at $\boldsymbol{\xi} =$ constant with the relation

$$\left.\frac{\partial U_j}{\partial t}\right|_{\mathrm{x}} = \left.\frac{\partial U_j}{\partial t}\right|_{\boldsymbol{\xi}} - \upsilon_k^*\frac{\partial U_j}{\partial x_k}. \tag{7}$$

So, the temporal derivative term in Equation (6) can be transformed using Equation (3) as follows:

$$\begin{aligned} J\left.\frac{\partial U_j}{\partial t}\right|_{\mathrm{x}} &= J\left.\frac{\partial U_j}{\partial t}\right|_{\boldsymbol{\xi}} - J\upsilon_k^*\frac{\partial U_j}{\partial x_k}, \\ &= \left.\frac{\partial (JU_j)}{\partial t}\right|_{\boldsymbol{\xi}} - JU_j\frac{\partial \upsilon_k^*}{\partial x_k} - J\upsilon_k^*\frac{\partial U_j}{\partial x_k}, \\ &= \left.\frac{\partial (JU_j)}{\partial t}\right|_{\boldsymbol{\xi}} - J\frac{\partial (U_j)\upsilon_k^*}{\partial x_k}. \end{aligned} \tag{8}$$

Replacing Equation (8) in Equation (6),

$$\int_{\Omega^\xi} w(\boldsymbol{\xi})\left.\frac{\partial}{\partial t}(JU_j)\right|_{\boldsymbol{\xi}}\mathrm{d}\Omega^\xi + \int_{\Omega^\xi}\left(\mathcal{F}_{jk}^c - \upsilon_k^* U_j - \mathcal{F}_{jk}^d\right)_{,k} w(\xi)J\,\mathrm{d}\Omega^\xi = 0. \tag{9}$$

The temporal derivative can be commuted with the integral and the weighting function because both do not depend on time so that

$$\frac{\mathrm{d}}{\mathrm{d}t}\left(\int_{\Omega^\xi} w\,JU_j\,\mathrm{d}\Omega^\xi\right) + \int_{\Omega^\xi}\left(\mathcal{F}_{jk}^c - \upsilon_k^* U_j - \mathcal{F}_{jk}^d\right)_{,k} wJ\,\mathrm{d}\Omega^\xi = 0, \tag{10}$$

and the integrals can be brought back to the $\Omega^t$ domain

$$\frac{\mathrm{d}}{\mathrm{d}t}\left(\int_{\Omega^t} w\,U_j\,\mathrm{d}\Omega^t\right) + \int_{\Omega^t}\left(\mathcal{F}_{jk}^c - \upsilon_k^* U_j - \mathcal{F}_{jk}^d\right)_{,k} w\,\mathrm{d}\Omega^t = 0. \tag{11}$$

The variational formulation can be obtained by integrating by parts so that

$$\frac{\mathrm{d}}{\mathrm{d}t}\left(H(w,U)\right) + F(w,U) = 0, \tag{12}$$





DOI: 10.1002/fld

where

$$
\begin{aligned}
H(w,U) &= \int_{\Omega^t} w\, U_j \mathrm{d}\Omega^t,\\
F(w,U) &= A(w,U) + B(w,U) + S(w,U),\\
A(w,U) &= -\int_{\Omega^t} \left(\mathcal{F}^c_{jk} - \upsilon^*_k U_j - \mathcal{F}^d_{jk}\right) w_{,k}\, \mathrm{d}\Omega^t,\\
B(w,U) &= \int_{\Gamma^t} \left(\mathcal{F}^c_{jk} - \upsilon^*_k U_j - \mathcal{F}^d_{jk}\right) n_k w\, \mathrm{d}\Gamma,
\end{aligned}
\tag{13}
$$

$\Gamma^t$ is the boundary of $\Omega^t$, and $n_k$ is its unit normal vector pointing to the exterior of $\Omega$. Also, a consistent stabilization term $S(w,U)$ is included to avoid numerical problems for advection dominated problems [24].

Finally, Equation (11) is discretized in time with the *trapezoidal rule* (application to the BDF will be described later)

$$
\begin{aligned}
H(w,U^{n+1}) - H(w,U^n) &= -\int_{t^n}^{t^{n+1}} F(w,U^{t'})\mathrm{d}t',\\
&\approx -\Delta t\, F(w,U^{n+\theta}).
\end{aligned}
\tag{14}
$$

with $0 \leqslant \theta \leqslant 1$ and being $U^{n+\theta}$ defined as

$$
U^{n+\theta} = (1-\theta)U_n + \theta U^{n+1}. \tag{15}
$$

During the time step, it is assumed that the nodal points move with constant velocity, that is,

$$
\left.
\begin{aligned}
\upsilon^*_k(\boldsymbol{\xi}) &= \frac{x_k(\boldsymbol{\xi},t^{n+1}) - x_k(\boldsymbol{\xi},t^n)}{\Delta t},\\
x_k(\boldsymbol{\xi},t) &= x_k(\boldsymbol{\xi},t^n) + (t-t^n)\upsilon^*_k(\boldsymbol{\xi}),
\end{aligned}
\right\}, \qquad \text{for } t^n \leqslant t \leqslant t^{n+1}. \tag{16}
$$

### 2.1. Discrete geometric conservation law condition

A discrete formulation is said to satisfy the DGCL condition if it solves exactly a constant state regime, that is, not depending on space or time for a general mesh movement $\mathbf{x}(\boldsymbol{\xi},t)$. As was mentioned in Section 1, the effect of the DGCL in the precision and numerical stability of the scheme is an open discussion, but in several works [14, 16], it is recommended to employ numerical schemes that satisfy the DGCL. This may help in improving the precision and the stability.

By replacing $U_j$ = constant and after some manipulations, it can be shown that the DGCL is satisfied if

$$
\int_{\Omega^{n+1}} w\, \mathrm{d}\Omega - \int_{\Omega^n} w\, \mathrm{d}\Omega = \Delta t \int_{\Omega^{n+\theta}} \upsilon^*_k w_{,k}\, \mathrm{d}\Omega. \tag{17}
$$

A similar restriction holds for the boundary term. The stabilization term $S(w,U)$ normally satisfies automatically the DGCL because it involves gradients of the state and then it is null for a constant state.

Note that this previous equation holds if the right-hand side is evaluated as an integral instead of being evaluated at $t^{n+\theta}$, that is, the DGCL error comes from the approximation that was made in Equation (14), that is, it is always true that

$$
\int_{\Omega^{n+1}} w\, \mathrm{d}\Omega - \int_{\Omega^n} w\, \mathrm{d}\Omega = \int_{t^n}^{t^{n+1}} \left\{\int_{\Omega^t} \upsilon^*_k w_{,k}\, \mathrm{d}\Omega\right\} \mathrm{d}t. \tag{18}
$$





DOI: 10.1002/fld

Consider the integrand in the right-hand side. Transforming to the reference domain $\Omega^\xi$, we obtain

$$\begin{aligned}\int_{t^n}^{t^{n+1}} \left\{\int_{\Omega^t} \upsilon_k^* \, w_{,k} \, \mathrm{d}\Omega\right\} \mathrm{d}t &= \int_{t^n}^{t^{n+1}} \left\{\int_{\Omega^\xi} \upsilon_k^* \frac{\partial w}{\partial \xi_l} \frac{\partial \xi_l}{\partial x_k} J \, \mathrm{d}\Omega^\xi\right\} \mathrm{d}t, \\ &= \int_{\Omega^\xi} \upsilon_k^* \frac{\partial w}{\partial \xi_l} \int_{t^n}^{t^{n+1}} \left(\frac{\partial \xi_l}{\partial x_k} J\right)^t \mathrm{d}t \, \mathrm{d}\Omega^\xi, \\ &= \int_{\Omega^\xi} \upsilon_k^* g_k^{n+\theta} J^{n+\theta} \, \mathrm{d}\Omega^\xi. \\ &= \int_{\Omega^{n+\theta}} \upsilon_k^* g_k^{n+\theta} \, \mathrm{d}\Omega,\end{aligned} \tag{19}$$

where $g_k$ is an *averaged interpolation function gradient*

$$\begin{aligned} g_k^{n+\theta} &= (J^{n+\theta})^{-1} \bar{Q}_{lk}^{n+1/2} \frac{\partial w}{\partial \xi_l}, \\ \bar{Q}_{lk}^{n+1/2} &= \int_{t^n}^{t^{n+1}} Q_{lk}^t \, \mathrm{d}t, \\ Q_{lk}^t &= \left(J \frac{\partial \xi_l}{\partial x_k}\right)^t. \end{aligned} \tag{20}$$

The proposed scheme is then to replace the $A(w, U^{n+\theta})$ operator in Equation (14) by

$$A^{\mathrm{GCL}}(w, U^{n+\theta}) = -\int_{\Omega^{n+\theta}} \left[\mathcal{F}_{jk}^c - \upsilon_k^* U_j - \mathcal{F}_{jk}^d\right]\Big|_{t^{n+\theta}} g_k^{n+\theta} \mathrm{d}\Omega, \tag{21}$$

A similar modification must be introduced in the boundary term $B(w, U)$; this will be explained later in Section 2.3. It is easy to check that with this modification, the scheme is DGCL compliant for all $\theta$.

### 2.2. *Evaluation of the average interpolation function gradient*

Because of Equation (16), each component $x_k$ is a linear function of time inside the time step, then the spatial derivatives $(\partial x_k/\partial \xi_l)$ are also linear functions and the determinant $J$ is a polynomial of degree $n_d$. Also, the components of the inverse transformation $\boldsymbol{\xi} \to \mathrm{x}$ can be determined from the inverse of the direct transformation $\mathrm{x} \to \boldsymbol{\xi}$ as

$$\begin{aligned} \frac{\partial \xi_l}{\partial x_k} &= \left(\frac{\partial \mathrm{x}}{\partial \boldsymbol{\xi}}\right)_{lk}^{-1}, \\ J \frac{\partial \xi_l}{\partial x_k} &= (-1)^{k+l} \text{ minor } \left(\frac{\partial \mathrm{x}}{\partial \boldsymbol{\xi}}\right)_{kl}, \end{aligned} \tag{22}$$

where minor $(\mathbf{A})_{ij}$ is the determinant of the submatrix of $\mathbf{A}$ when row $i$ and column $j$ have been eliminated. Then, the minors are polynomials of order $n_d - 1$ and so are the entries of $J(\partial \xi_l/\partial x_k)$ that are the integrands in Equation (20).

As a check, well-known results about the compliance of the DGCL with the trapezoidal rule will be verified. The DGCL is satisfied if the integration rule used to approximate the time integral in Equation (20) is exact, for instance, $\theta = 1/2$ satisfies the DGCL in 2D because the integrand is linear and the trapezoidal rule reduces to the midpoint rule. In addition, DGCL is satisfied in 1D for any $0 \leqslant \theta \leqslant 1$ and for none in 3D. The point is that using $\theta = 1/2$ (Crank–Nicolson) is restrictive, and there is no $\theta$ that satisfies the DGCL in 3D so that the method proposed here uses a higher order time integration for Equation (20) so that the DGCL is satisfied for an arbitrary $\theta$ in any dimension. The method can be extended easily to other temporal integration schemes (Section 2.4).

For instance, the Gauss integration method can be used. Normally the Jacobians and the determinants are known at $t^n$ and $t^{n+1}$ because they are needed for the computation of the temporal





DOI: 10.1002/fld

term (the right-hand side in Equation (14)), so perhaps it is better to use the Gauss–Lobatto version, which includes the extremes of the interval. The Gauss–Lobatto method integrates exactly polynomials of up to degree $2n-3$, where $n$ is the number of integration points so that it suffices to use the extreme points for simplices in $n_d = 2$ and to add a point at the center of the interval for $n_d = 3$, that is,

$$g_k^{n+\theta} = \begin{cases} \dfrac{\Delta t}{2J^{n+\theta}}\left[Q_{lk}^n + Q_{lk}^{n+1}\right]\dfrac{\partial w}{\partial \xi_l}, & \text{in 2D,} \\ \dfrac{\Delta t}{6J^{n+\theta}}\left[Q_{lk}^n + 4Q_{lk}^{n+1/2} + Q_{lk}^{n+1}\right]\dfrac{\partial w}{\partial \xi_l}, & \text{in 3D,} \end{cases} \tag{23}$$

being $Q_{lk}^t$ defined in Equation (20).

### 2.3. Boundary term

The boundary term in Equation (13) can be brought to the reference domain as follows:

$$\begin{aligned} B(w,U) &= \int_{\partial\Gamma^t}\left[\mathcal{F}_{jk}^c - \upsilon_k^* U_j - \mathcal{F}_{jk}^d\right] w n_k \,\mathrm{d}\Gamma, \\ &= \int_{\partial\Gamma^\xi}\left[\mathcal{F}_{jk}^c - \upsilon_k^* U_j - \mathcal{F}_{jk}^d\right] w n_k J_\Gamma \,\mathrm{d}\Gamma^\xi, \end{aligned} \tag{24}$$

where $J_\Gamma$ is the Jacobian of the transformation between a surface element in $\Gamma^t$ and $\Gamma^\xi$. The DGCL is satisfied if the averaged normal vector is used, that is,

$$\begin{aligned} B^{\mathrm{GCL}}(w,U) &= \int_{\partial\Gamma^t}\left[\mathcal{F}_{jk}^c - \upsilon_k^* U_j - \mathcal{F}_{jk}^d\right] w \bar{n}_k \,\mathrm{d}\Gamma, \\ \bar{n}_k &= \frac{1}{J_\Gamma^\theta}\eta_k, \\ \eta_k &= \frac{1}{\Delta t}\int_{t^n}^{t^{n+1}} n_k J_\Gamma \,\mathrm{d}t. \end{aligned} \tag{25}$$

Regarding the evaluation of the integral for computing $\eta_k$, the considerations are very similar to those given in Section 2.2. The components of $n_k J_\Gamma$ are also polynomials of degree $n_d - 1$ in time. For instance in 3D, if $\mathrm{x}_1, \mathrm{x}_2$, and $\mathrm{x}_3$ are the nodes at the vertices of a triangle element (ordered counterclockwise when viewed from the exterior of the fluid) on the surface $\Gamma^t$, then

$$\mathrm{n}J_\Gamma = \frac{(\mathrm{x}_2 - \mathrm{x}_1)\times(\mathrm{x}_3 - \mathrm{x}_1)}{2|\Gamma^\xi|}, \tag{26}$$

where x denotes the vector cross product and $|\Gamma^\xi|$ is the area of the triangle in the reference coordinates. As the coordinates of the nodes are linear in time and $|\Gamma^\xi|$ is constant, the components of $n_k J_\Gamma$ are quadratic polynomials.

Then, the considerations about the number of points for the Gauss–Lobatto integration are the same as discussed before, that is, two integration points are enough to compute the integral in Equation (25) and three are needed in 3D.

### 2.4. Application to the backward differentiation formula

The BDF is another popular method for the integration of the system of ordinary differential equations [15, 16, 25]. By applying to Equation (12) gives

$$\frac{1}{\Delta t}\left({}^3\!/_2 H^{n+1} - 2H^n + {}^1\!/_2 H^{n-1}\right) = F(w, U^{n+1}). \tag{27}$$





DOI: 10.1002/fld

To apply the AJF, the right-hand side of Equation (27) must be rewritten as an integral over time. For this, note that for any differentiable function $X(t)$, we have

$$\begin{aligned} {}^3\!/_2 X^{n+1} - 2X^n + {}^1\!/_2 X^{n-1} &= {}^3\!/_2 (X^{n+1} - X^n) - {}^1\!/_2 (X^n - X^{n-1}), \\ &= {}^3\!/_2 \int_{t^n}^{t^{n+1}} \dot{X}\,\mathrm{d}t - {}^1\!/_2 \int_{t^n-1}^{t^n} \dot{X}\,\mathrm{d}t. \end{aligned} \tag{28}$$

If this relation is applied with the semidiscrete Equations (12) with $X = H$ and $\dot{X} = -F$, then the following relation is obtained

$$ {}^3\!/_2 H^{n+1} - 2H^n + {}^1\!/_2 H^{n-1} = -{}^3\!/_2 \int_{t^n}^{t^{n+1}} F(w, U^{t'})\,\mathrm{d}t' + {}^1\!/_2 \int_{t^{n-1}}^{t^n} F(w, U^{t'})\,\mathrm{d}t'. \tag{29}$$

The BDF integration method is obtained if the right-hand side in Equation (29) is replaced by the value of the integrand at $t^{n+1}$. The proposed method to satisfy the DGCL is to assume that the state in Equation (29) remains constant ($U(t) = U^{n+1}$) but the geometric quantities $\upsilon_k^*$ and $w_{,k}$ do not; therefore, these quantities must be averaged over time and some additional terms must be computed so that

$$ {}^3\!/_2 H^{n+1} - 2H^n + {}^1\!/_2 H^{n-1} = -\Delta t F^{\mathrm{BDF}}(w, U^{n+1}), \tag{30}$$

where

$$\begin{aligned} F^{\mathrm{BDF}}(w, U^{n+1}) &= A^{\mathrm{BDF}}(w, U^{n+1}) + B^{\mathrm{BDF}}(w, U^{n+1}) + S(w, U^{n+1}), \\ A^{\mathrm{BDF}}(w, U^{n+1}) &= -\int_{\Omega^{n+1}} \left[ \left( \mathcal{F}^c_{jk} - \mathcal{F}^d_{jk} \right)^{n+1} g_k^{n+1} - U_j^{n+1} r^{n+1} \right] \mathrm{d}\Omega, \\ B^{\mathrm{BDF}}(w, U^{n+1}) &= \int_{\partial\Gamma^t} \left[ \left( \mathcal{F}^c_{jk} - \mathcal{F}^d_{jk} \right) \beta_k^{n+1} - U_j^{n+1} s^{n+1} \right] w\,\mathrm{d}\Gamma, \end{aligned} \tag{31}$$

and $g_k$, $r$, $\beta_k$, and $s$ are time-averaged geometric quantities given by

$$\begin{aligned} g_k^{n+1} &= \frac{1}{J^{n+1}} \left( {}^3\!/_2 Q_{lk}^{n+1/2} - {}^1\!/_2 Q_{lk}^{n-1/2} \right) \frac{\partial w}{\partial \xi_l}, \\ r^{n+1} &= \frac{1}{J^{n+1}} \left( {}^3\!/_2 Q_{lk}^{n+1/2} \upsilon_k^{*n+1/2} - {}^1\!/_2 Q_{lk}^{n-1/2} \upsilon_k^{*n-1/2} \right) \frac{\partial w}{\partial \xi_l}, \\ \beta_k^{n+1} &= \frac{1}{J_\Gamma^{n+1}} \left( {}^3\!/_2 \eta_k^{n+1/2} - {}^1\!/_2 \eta_k^{n-1/2} \right), \\ s^{n+1} &= \frac{1}{J_\Gamma^{n+1}} \left( {}^3\!/_2 \eta_k^{n+1/2} \upsilon_k^{*n+1/2} - {}^1\!/_2 \eta_k^{n-1/2} \upsilon_k^{*n-1/2} \right), \\ \eta_k^{n+1/2} &= \frac{1}{\Delta t} \int_{t^n}^{t^{n+1}} n_k J_\Gamma\,\mathrm{d}t, \end{aligned} \tag{32}$$

and $\upsilon_k^{*n+1/2}$ is the (constant) velocity in the time step $[t^n, t^{n+1}]$. Regarding the computation of the averaged Jacobians $Q_{lk}^{n+1/2}$ and $\eta_k^{n+1/2}$, the rules are the same as before (Equations (20) and (25)) because their entries are polynomials of degree $n_d - 1$ within the time interval.





DOI: 10.1002/fld

## 3. NUMERICAL TESTS

In this section, a set of numerical tests are performed to validate the AJF proposed in Section 2.

### *3.1. Discrete geometric conservation law validation for 2D scalar diffusion problem with internal node movement*

For the sake of clarity, let us consider the scalar diffusion version of Equation (1).

$$\begin{aligned} \frac{\partial u}{\partial t} - \mu \Delta u = 0 \quad & \text{for } \mathbf{x} \in \Omega^{\mathrm{t}},\ \mathrm{t} \in (0, \mathrm{T}] \\ u = u_0 \quad & \text{for } \mathbf{x} \in \Omega^{0},\ \mathrm{t} = 0 \\ u = u_D \quad & \text{for } \mathbf{x} \in \partial\Omega^{\mathrm{t}},\ \mathrm{t} \in [0, \mathrm{T}] \end{aligned} \tag{33}$$

where $\mu$ is the constant diffusivity and $\Delta$ is the Laplacian operator.

To carry out the DGCL compliance test, problem (33) is solved on a unit square domain with $\mu = 0.01$ so that

$$\begin{aligned} u_t - 0.01\Delta u = 0 \quad & \text{for } \mathbf{x} \in \Omega^{\mathrm{t}}, \mathrm{t} \in (0, \mathrm{T}], \\ u_0 = 1 \quad & \text{for } \mathbf{x} \in \Omega^{0}, \mathrm{t} = 0, \\ u = 1 \quad & \text{for } \mathbf{x} \in \Gamma^{\mathrm{t}}, \mathrm{t} \in [0, \mathrm{T}], \end{aligned} \tag{34}$$

being the mesh deformed according to the following rule

$$\begin{aligned} \chi_1(\xi, t) &= x = \xi + 0.125 \sin(\pi\ t) \sin(2\pi\ \xi). \\ \chi_2(\eta, t) &= y = \eta + 0.125 \sin(\pi\ t) \sin(2\pi\ \eta). \end{aligned} \tag{35}$$

As was mentioned in Section 2.1, a discrete formulation is said to satisfy the DGCL condition if it solves exactly a constant state regime, that is, not depending on space or time for a general mesh movement $\mathbf{x}(\boldsymbol{\xi}, t)$.

F1 Figure 1 shows the reference domain and the deformed mesh for $t = 0.5$ [s] where the maximum deformation occurs.

The problem is solved using piecewise linear triangles for the spatial discretization, a piecewise linear interpolation of the mesh movement, and for the time integration the *backward Euler* (BE, $\theta = 1$), *Crank–Nicolson* (CN, $\theta = 0.5$), and *Galerkin* (GA, $\theta = 2/3$) schemes are considered F2 with $\Delta t = \{0.15, 0.1, 0.05, 0.025\}$. Figure 2 reports the error $||u_h - u||_{L^2(\Omega_t)}$ for three periods of oscillation, using the time integration methods and time steps mentioned previously. The error must be null to machine precision over time for a DGCL compliant scheme.

A numerical error is introduced when using the backward Euler or Garlerkin scheme because of a F3 lack in DGCL compliance for 2D problems. In Figure 3, the solution for times $t = \{0.1, 2.4, 5.4\}$ [s]

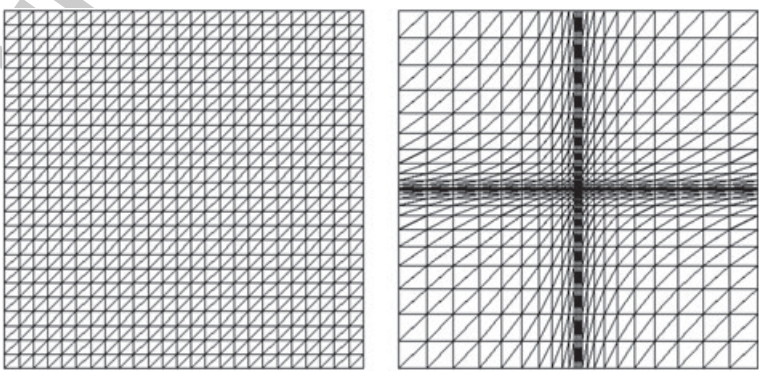

Figure 1. Reference and deformed mesh.





DOI: 10.1002/fld

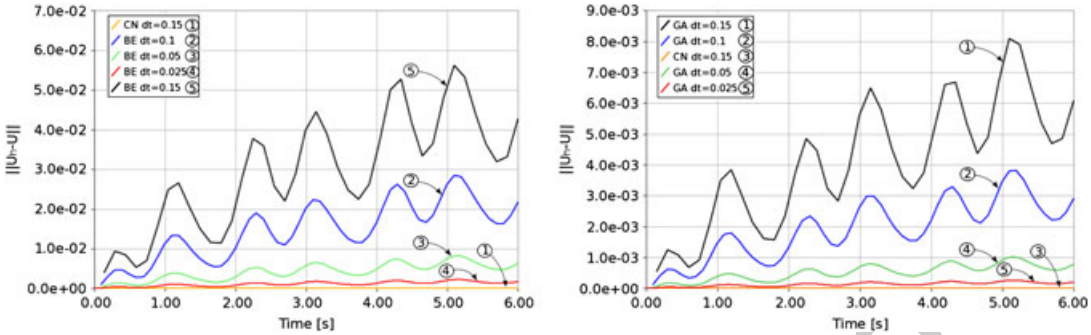


Figure 2. $||u_h - u||_{L^2(\Omega_t)}$ for Garlerkin (GA) and backward Euler (BE) schemes compared with Crank–Nicolson (CN).



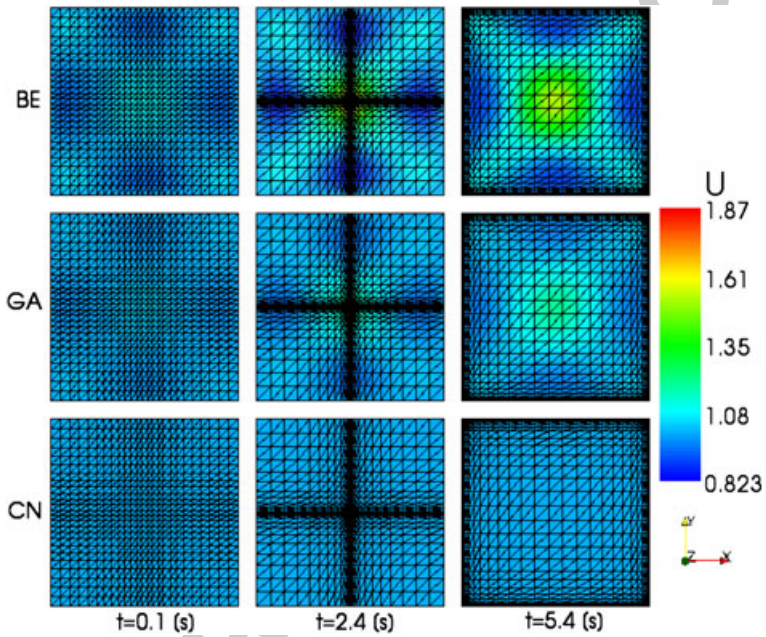


Figure 3. Solution for the backward Euler (BE), Galerkin (GA), and Crank–Nicolson (CN) schemes.

is shown for the three different integration schemes. The error related to the constant solution is located in the zones of the domain where the element deformation is higher, as in the center and the corners.

Now, if the AJF is used, all these three time integration schemes are DGCL compliant, so the error remains null to machine precision (Figure 4). F4

### 3.2. *Discrete geometric conservation law validation for 2D scalar diffusion problem with a periodic expansion and contraction of the domain*

In this test case, problem (33) is solved in a unit square domain with $\mu = 0.1$ so that

$$\begin{aligned} u_t - 0.1\Delta u &= 0 \quad \text{for } \mathbf{x} \in \Omega^{\mathrm{t}}, \mathrm{t} \in (0, \mathrm{T}], \\ u_0 &= 1 \quad \text{for } \mathbf{x} \in \Omega^0, \mathrm{t} = 0, \\ u &= 1 \quad \text{for } \mathbf{x} \in \partial\Omega^{\mathrm{t}}, \mathrm{t} \in [0, \mathrm{T}], \end{aligned} \tag{36}$$

being the domain deformed according to the following rule

$$\chi(\xi, t) = (2 - \cos(20\pi t))\xi. \tag{37}$$



DOI: 10.1002/fld

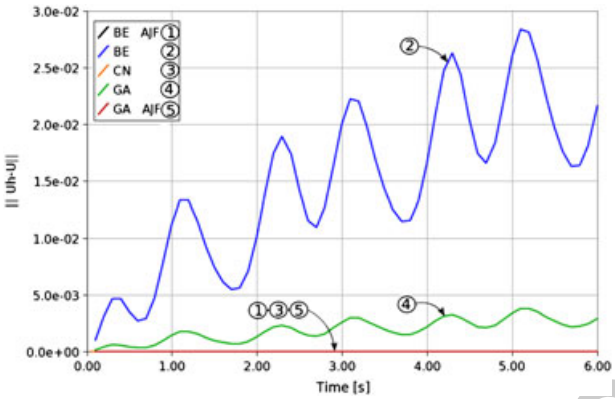


Figure 4. Errors using the averaged Jacobian formulation (AJF) and no averaged Jacobian formulation for $\Delta t = 0.1$ [s].

This deformation rule represents a periodic expansion and contraction of the domain as it is shown in Figure 5 for $t = \{0, 0.03, 0.05\}$ [s].

As in the previous case, a numerical error is introduced when using the backward Euler or Garlerkin scheme because of a lack in DGCL compliance for 2D problems; but when the AJF is used, all the time integration schemes are DGCL compliant.

In Figure 6, the error $||u_h - u||_{L^2(\Omega_t)}$ in the solution is reported for four periods of oscillation.

### *3.3. Discrete geometric conservation law validation for 3D scalar diffusion problem with a periodic expansion and contraction of the domain*

In this section, the AJF is validated for 3D problems. The initial test is the extension to 3D of problem (36) and the mesh moving rule (37). It is solved using piecewise linear tetrahedral for the spatial discretization, a piecewise linear interpolation of the mesh movement, and for the time integration, the backward Euler ($\theta = 1$), Crank–Nicolson ($\theta = 0.5$), and Garlerkin ($\theta = 2/3$) schemes.

Figure 7 shows the deformed domain for $t = \{0, 0.03, 0.05\}$ [s], and Figure 8 reports the error $||u_h - u||_{L^2(\Omega_t)}$ for four periods of oscillation. When the AJF is used, the error remains null to machine precision because the scheme is DGCL compliant.

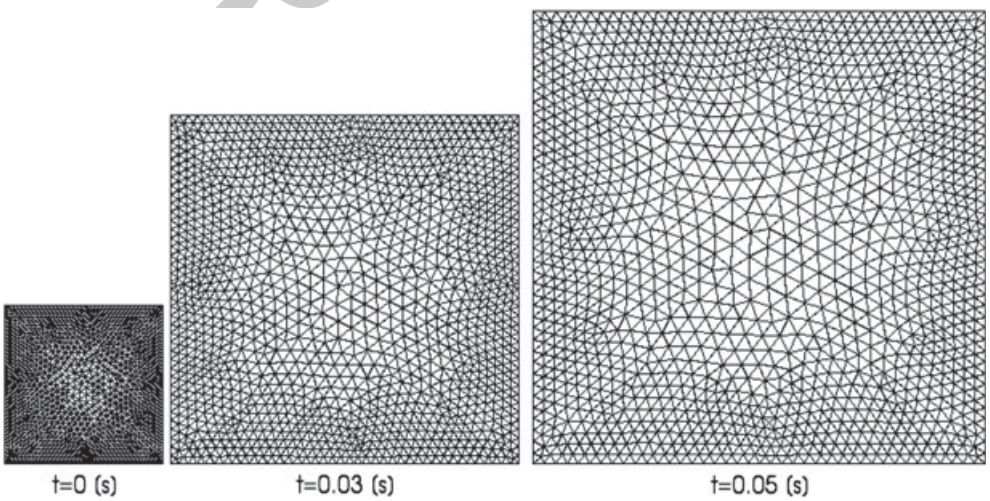


Figure 5. Deformed domain.





DOI: 10.1002/fld

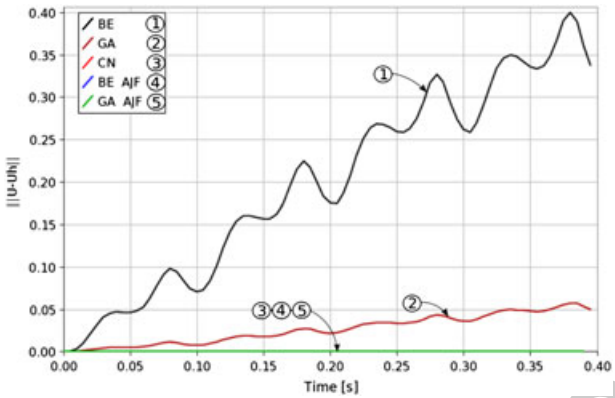


Figure 6. $||u_h - u||_{L^2(\Omega_t)}$ for backward Euler (BE), Galerkin (GA), and Crank–Nicolson (CN) schemes for $\Delta t = 0.005$ [s].

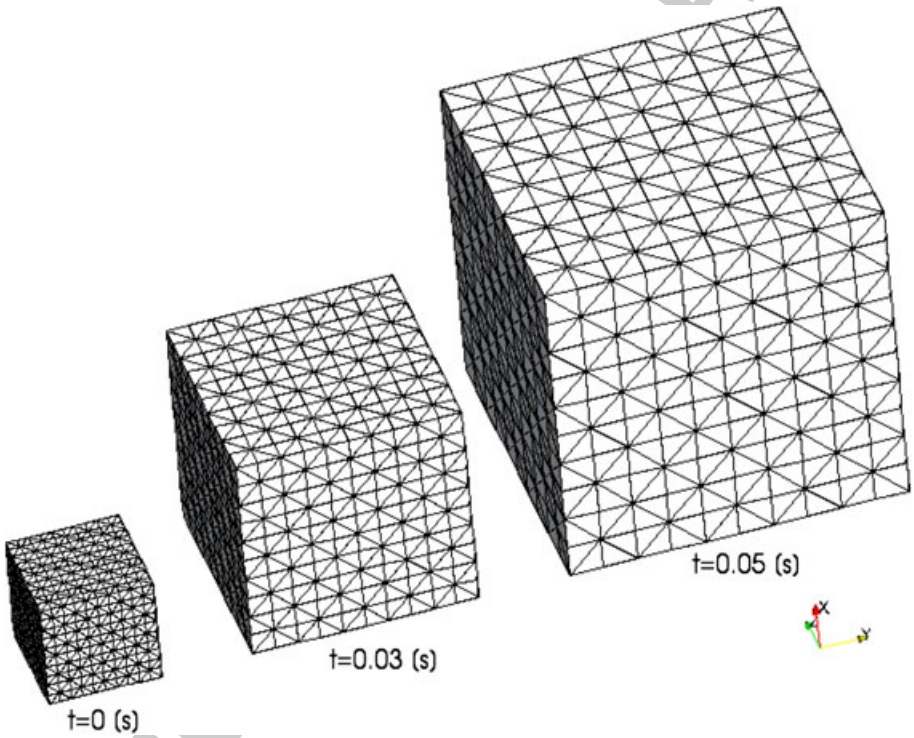


Figure 7. Deformed domain.

### 3.4. *Discrete geometric conservation law validation for 3D scalar diffusion problem with internal node movement*

This test is the extension to 3D of problem (34) and the deformation rule (35). It is solved using piecewise linear tetrahedral for the spatial discretization, a piecewise linear interpolation of the mesh movement, and for the time integration, the backward Euler ($\theta = 1$), Crank–Nicolson ($\theta = 0.5$), and Garlerkin ($\theta = 2/3$) schemes.

Figure 9 shows the deformed mesh for $t = \{0, 0.5, 1.5\}$ [s], and Figure 10 reports the error $||u_h - u||_{L^2(\Omega_t)}$. F9 F10

A numerical error is introduced when using any of the $\theta$-family scheme in 3D problems because of a lack in GCL compliance. In Figure 11, the solution for times $t = \{0.1, 2.4, 5.4\}$ [s] is shown for the backward Euler scheme. The error with respect to the constant solution are localized in the F11



DOI: 10.1002/fld

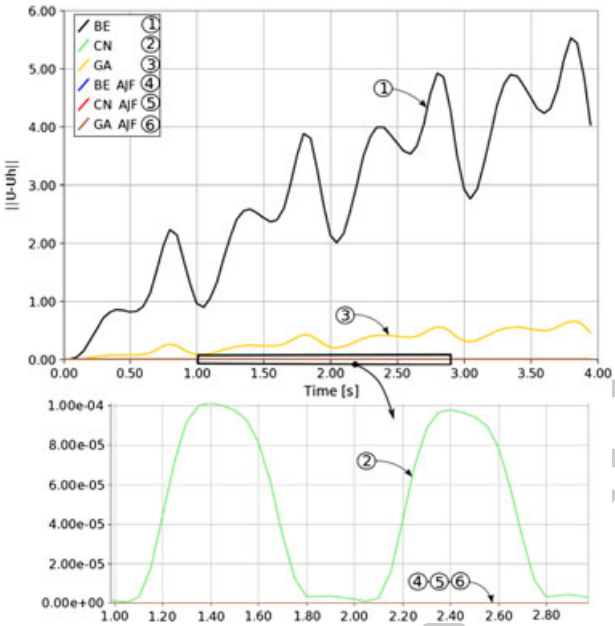


Figure 8. Errors for averaged Jacobian formulation (AJF) and no averaged Jacobian formulation for $\Delta t = 0.005$ [s].

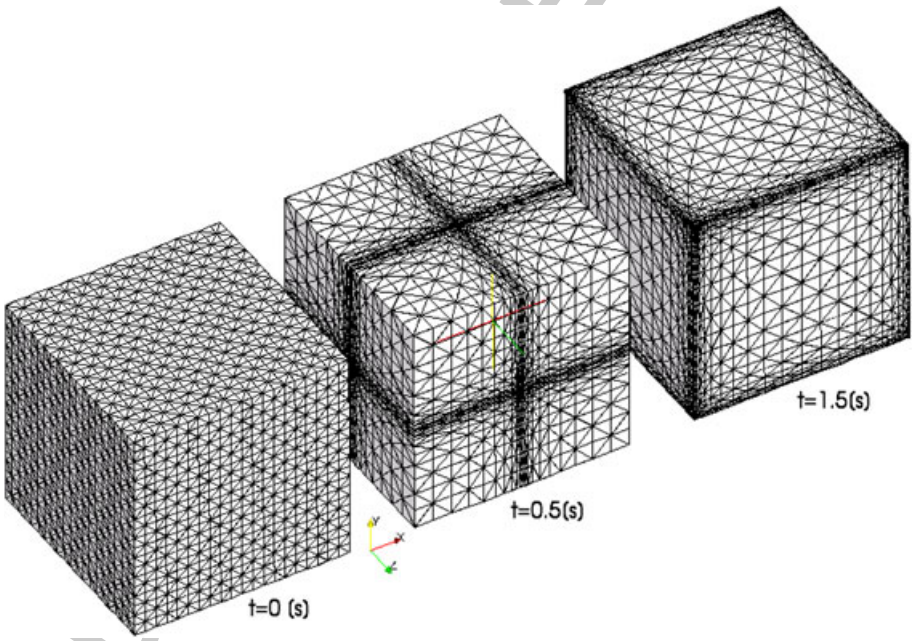


Figure 9. Deformed mesh.

zones of the domain where the element deformation is higher, as in the center. But when the AJF is used, the error remains null to machine precision because the scheme is DGCL compliant.

### 3.5. *Moving an internal cylinder*

This example consists of an external cylinder of radius $R_2$, which contains an internal smaller cylinder of radius $R_1$ and performs an harmonic motion of amplitude $d_0$ with an angular frequency $\omega$, that is, the instantaneous displacement of the center of the internal cylinder $d$ is



DOI: 10.1002/fld

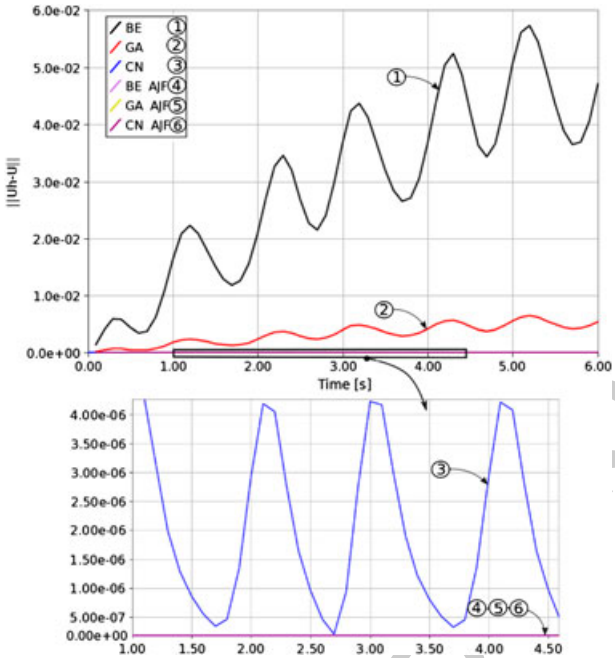


Figure 10. $||u_h - u||_{L^2(\Omega_t)}$ for backward Euler (BE), Galerkin (GA), and Crank–Nicolson (CN) schemes for $\Delta t = 0.005$ [s].

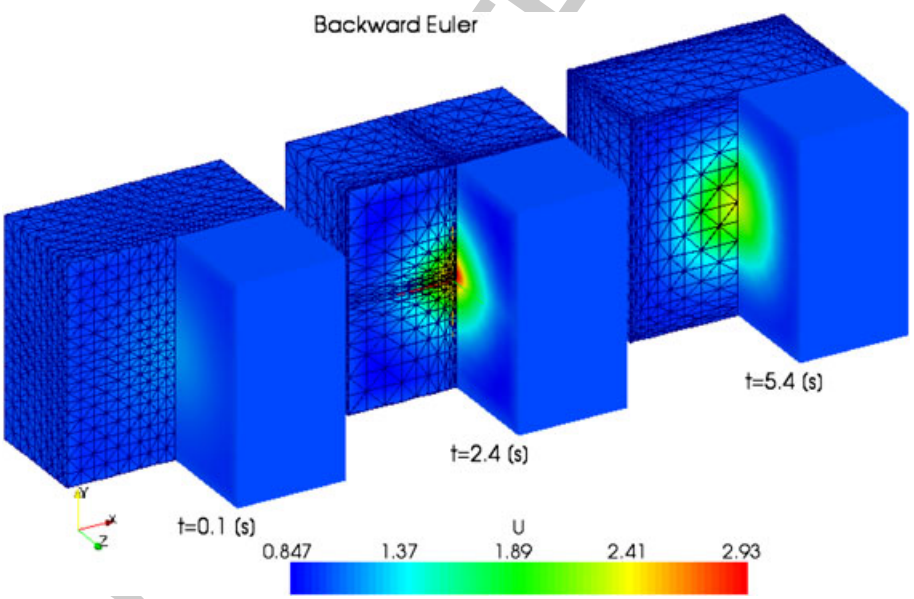


Figure 11. Solution for the backward Euler scheme.

$$d(t) = d_0 \sin(\omega t) \tag{38}$$

In this example, an orthogonal mapping can be found between the reference domain where the two cylinders are concentric and the general case where they are eccentric (cf. Appendix A). So, instead of using a mesh movement strategy for distorting the mesh, the instantaneous mesh is obtained by applying the said transformation to the position of the nodes of a mesh in the reference domain.

In this test, the parameters used were $R_2 = 2$, $R_1 = 1$, $\omega = 1.047$, and $d_0 = 0.7$ and the maximum velocity of the inner cylinder is $v_{\max} = 0.733$. The domain was discretized with 10 elements in the radial direction and 96 elements in the perimeter using linear triangular elements


Color Online, B&W in Print



DOI: 10.1002/fld

(Figure 12). The dimensionless equations of a viscous compressible flow were solved in the interior of the domain using the backward Euler time integration scheme, varying the Courant number between 2 and 0.025. The fluid properties used in the simulation are, $\rho_{\text{ref}} = 1$, $p_{\text{ref}} = 1$, $\gamma = 1.4$, and $\nu = 0.001$. At the boundary of the inner cylinder is imposed the velocities that result from the imposed movement, and at the boundary of outer cylinder is imposed a no-slip condition.

To analyze the numerical error introduced because of a lack in DGGL compliance, the density on a fixed spatial point with coordinates $\mathbf{x} = (1.8, 0.2)$ was plotted in Figures 13–15 for four periods of oscillation.

As the time step is reduced, the differences between the solutions obtained with the AJF and without decreases, as was stated in the previous examples. In the results corresponding to Co=2, the

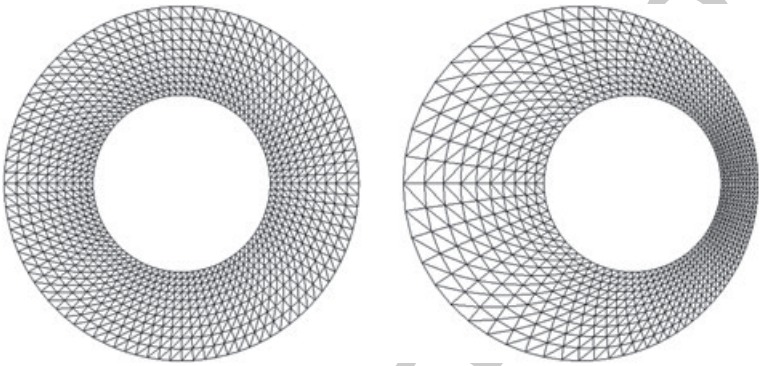

Figure 12. Initial mesh and maximum displacement mesh.

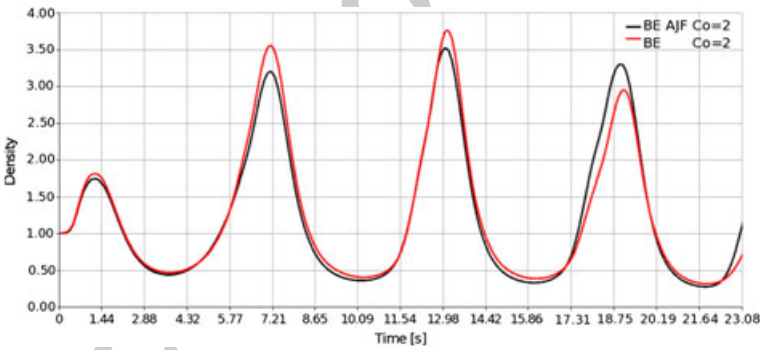


Figure 13. Density using the averaged Jacobian formulation (AJF) and no averaged Jacobian formulation for Co = 2.

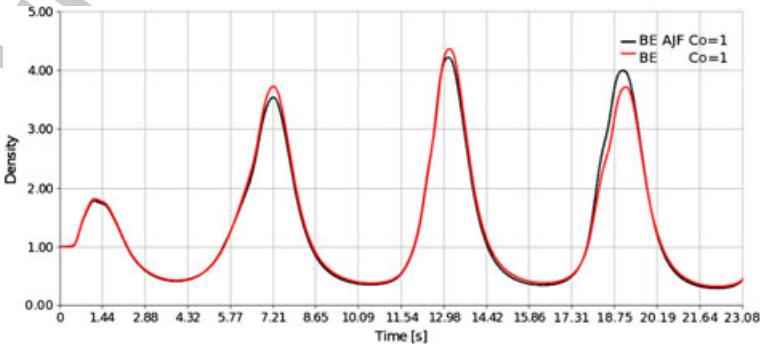


Figure 14. Density using the averaged Jacobian formulation (AJF) and no averaged Jacobian formulation for Co = 1.





DOI: 10.1002/fld

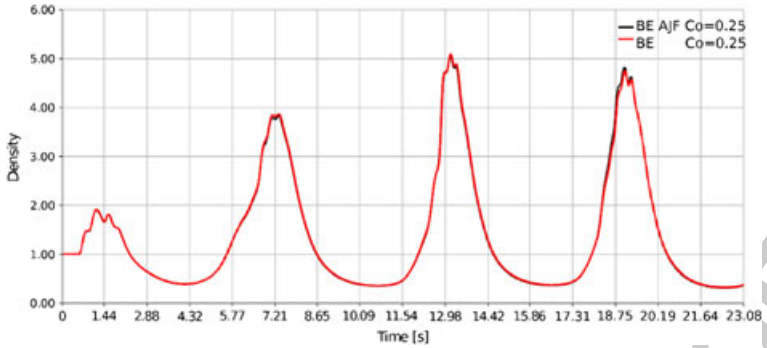


Figure 15. Density using the averaged Jacobian formulation (AJF) and no averaged Jacobian formulation for Co = 0.25.

difference between both solutions are significative, whereas in the results corresponding to Co=0.25 are negligible.

In Figure 16, the pressure distribution in the domain for different positions of the inner cylinder is shown. The domain was discretized with 35 elements in the radial direction and 342 elements in the perimeter using triangular elements. The pressure increase in the compressed region induces a fluid motion towards the opposite side as shown by the velocity vectors of the figure.

## 4. CONCLUSIONS

The proposed methodology guarantees compliance with the DGCL criterion in the context of the ALE solutions of general advective–diffusive systems using classical temporal integration schemes and simplicial finite elements in 2D and 3D. Detailed expressions for the computation of the averaged Jacobians and its application to the $\theta$ family and the three-point BDF schemes were given. Also, to validate the AJF, a set of typical numerical tests for linear scalar advective–diffusive and Euler models were performed.

Unlike to previous work, this new methodology is not based on proposing a new temporal integration scheme and computing a set of unknown numerical coefficients to achieve compliancy with the

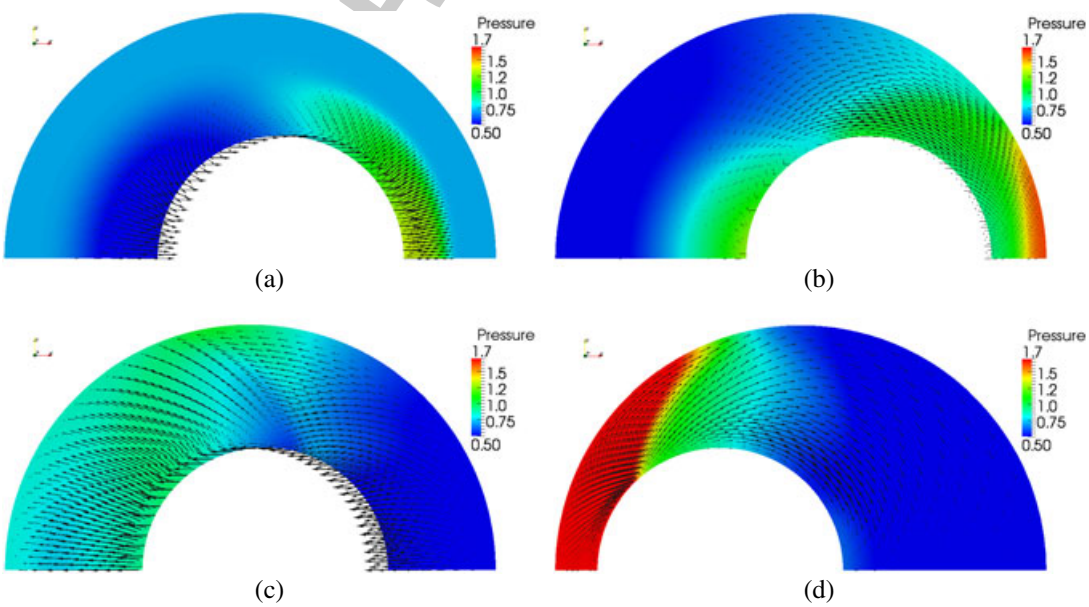


Figure 16. Pressure at different positions of the inner cylinder.





DOI: 10.1002/fld

DGCL but rather by averaging some geometrical quantities. These averages are computed exactly using the Gauss–Lobatto numerical quadrature. The averaging process of the Jacobian must be introduced in the volume terms as well as in the boundary terms. The added cost is negligible and only involves a few changes at the elemental routine level.

## APPENDIX A. ORTHOGONAL MAPPING

The transformation between the current domain and the reference domain can be described as the composition of two conformal mappings ($z \to w \to v$) and a third orthogonal (but nonconformal) mapping ($v \to u$). Here $u$, $v$, $w$, and $z$ are complex variables. The $z$-plane (Figure A.1(a)) is the physical plane with the current position (eccentric) of the inner cylinder. The region in the $z$-plane is

$$\Omega_z(t) = \{z \in \mathbb{C} / |z| < R_2 \text{ and } |z - d(t)| > R_1\} \tag{A.1}$$

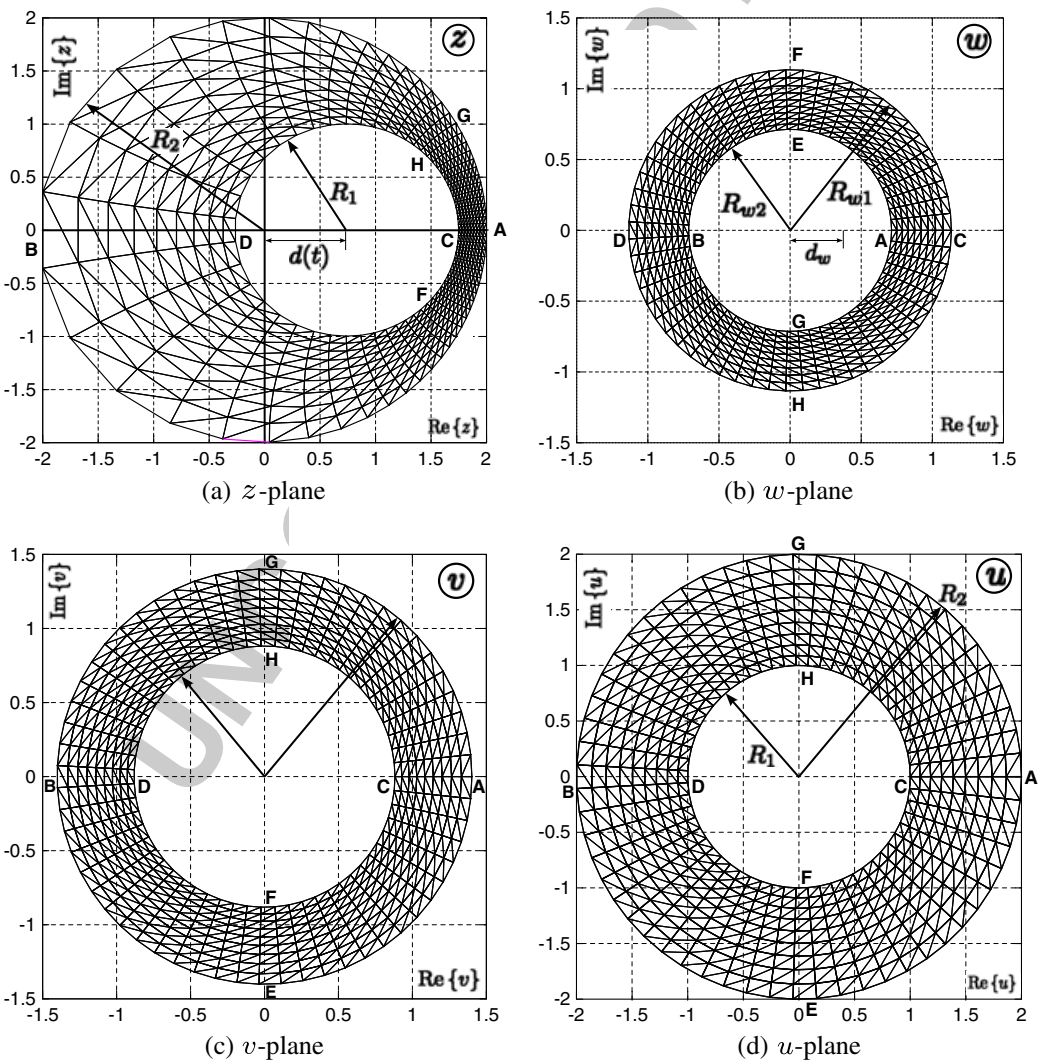


(a) $z$-plane (b) $w$-plane

(c) $v$-plane (d) $u$-plane

Q2 Figure A.1. ■■.





DOI: 10.1002/fld

The key transformation is the inversion

$$z = \frac{1}{w + d_w} + z_0 \tag{A.2}$$

which transforms the circular annulus

$$\Omega_w = \{w \in \mathbb{C} \ / \ R_{w2} \leqslant |w| \leqslant R_{w1}\} \tag{A.3}$$

in the $w$-plane onto $\Omega_z$. As it is an inversion transformation, it maps lines and circles onto lines and circles. The real parameters of the transformation $R_{w1}, R_{w2}, d_w, z_0$ are unknown, but they can be easily found by adjusting the points $A$, $B$, $C$, and $D$ so that the radiuses in the $z$-plane are $R_1$ and $R_2$, as required. The coordinates of these points in the $w$-plane are

$$\begin{aligned} w_A &= R_{w2}, \\ w_B &= -R_{w2}, \\ w_C &= R_{w1}, \\ w_D &= -R_{w1}. \end{aligned} \tag{A.4}$$

and then, using transformation (A.2), their $z$-coordinates are

$$\begin{aligned} z_A &= \frac{1}{d_w + R_{w2}} + z_0, \\ z_B &= \frac{1}{d_w - R_{w2}} + z_0, \\ z_C &= \frac{1}{d_w + R_{w1}} + z_0, \\ z_D &= \frac{1}{d_w - R_{w1}} + z_0. \end{aligned} \tag{A.5}$$

Then, we arrive to the following equations

$$\begin{aligned} z_A - z_B &= 2R_2, \\ z_C - z_D &= 2R_1, \\ z_{c1} - z_{c2} &= \frac{z_C + z_D}{2} - \frac{z_A + z_B}{2} = d. \end{aligned} \tag{A.6}$$

The last equation comes from the requirement that the center $z_{c1}$ of the internal cylinder must be shifted a distance $d$ from the center $z_{c2}$ of the external cylinder. Replacing with the expressions for the $z$-coordinates given in Equation (A.5), we arrive to the equations

$$\begin{aligned} \frac{1}{d_w + R_{w2}} - \frac{1}{d_w - R_{w2}} &= 2R_2, \\ \frac{1}{d_w + R_{w1}} - \frac{1}{d_w - R_{w1}} &= 2R_1, \\ \frac{1}{d_w + R_{w2}} + \frac{1}{d_w - R_{w2}} - \frac{1}{d_w + R_{w1}} - \frac{1}{d_w - R_{w1}} &= 2d. \end{aligned} \tag{A.7}$$

which is a system of three nonlinear equations that can be solved for $R_{w1}$, $R_{w2}$, and $d_w$ in terms of $R_1$, $R_2$, and $d$. The system can be solved with the Newton–Raphson method, for instance. Note that the fourth parameter $z_0$ does not enter in the equations. Once these three parameters are found, $z_0$ can be easily found from the requirement that the external cylinder must be centered at $\mathrm{Re}\,\{z\} = 0$, that is,

$$z_{c2} = \frac{z_A + z_B}{2} + z_0 = 0, \tag{A.8}$$





DOI: 10.1002/fld

from where

$$z_0 = -\frac{z_A + z_B}{2}. \tag{A.9}$$

Once the $z - w$ transformation is known, the other two are easily found. Note that, because of the inversion, the internal radius in the $\Omega_w$ domain is mapped onto the external radius in the $\Omega_z$ domain, and vice versa. Then, a second inversion is performed

$$w = \frac{1}{v}, \tag{A.10}$$

and the resulting $\Omega_v$ domain is a circular annulus

$$\Omega_v = \left\{ v \in \mathbb{C}^2 \ / \ R_{v1} \leqslant |v| \leqslant R_{v2} \right\}\}. \tag{A.11}$$

with $R_{v1} = 1/R_{w1}$ and $R_{v2} = 1/R_{w2}$. Finally, the transformation $u - v$ is orthogonal (but nonconformal) that maps linearly the radius so as to map the $\Omega_v$ domain onto the reference domain

$$\Omega_u = \Omega_z(d = 0) = \left\{ u \in \mathbb{C}^2 \ / \ R_1 \leqslant |u| \leqslant R_2 \right\}\}. \tag{A.12}$$

The transformation is better described in terms of polar coordinates $v = |v|e^{i\phi_v}$, $u = |u|e^{i\phi_u}$ as follows

$$\begin{aligned} \phi_v &= \phi_u, \\ |v| &= R_{v1} + \frac{|u| - R_1}{R_2 - R_1}(R_{v2} - R_{v1}). \end{aligned} \tag{A.13}$$

Computationally, the process is as follows. At a certain time $t$, the nodes' position must be determined; first, the parameters of the transformation are determined from Equation (A.6). Then, given the coordinates of the node in the reference domain $u$, the successive transformations (A.13), (A.10), and (A.2) are applied, and the coordinates of the node in the actual position of the mesh $z$ are obtained.

ACKNOWLEDGEMENTS

This work has received financial support from the Consejo Nacional de Investigaciones Científicas y Técnicas (CONICET, Argentina, grant PIP 5271/05), the Universidad Nacional del Litoral (UNL, Argentina, grant CAI+D 2009 65/334), and the Agencia Nacional de Promoción Científica y Tecnológica (ANPCyT, Argentina, grants PICT 01141/2007, PICT 2008-0270 'Jóvenes Investigadores', PICT 1506/2006). Extensive use of freely distributed software such as GNU/Linux OS, MPICH, PETSc, Metis, Octave, ParaView, and many others is carried out in this work.

REFERENCES

1. Tezduyar TE, Sathe S, Schwaab M, Conklin BS. Arterial fluid mechanics modeling with the stabilized space-time fluid-structure interaction technique. *International Journal for Numerical Methods in Fluids* 2008; **57**(7):601–609.
2. Lefrancois E, Dhatt G, Vandromme D. Fluid–structure interaction with application to rocket engines. *International Journal for Numerical Methods in Fluids* 1999; **30**:865–895.
3. Storti MA, Nigro N, Paz RR, Dalcín DL. Strong coupling strategy for fluid structure interaction problem in supersonic regime via fixed point iteration. *Journal of Sound and Vibration* 2009; **30**:859–877.
4. Garelli L, Paz RR, Storti MA. Fluid–structure interaction study of the start-up of a rocket engine nozzle. *Computers & Fluids* 2010; **39**(7):1208–1218.
5. Noh WF. A time-dependent, two space dimensional, coupled Eulerian–Lagrangian code. *Methods in Computational Physics* 1964; **3**:117–179.
6. Hirt CW, Amsden AA, Cook JL. An arbitrary Lagrangian–Eulerian computing method for all flow speeds. *Journal of Computational Physics* 1974; **14**(3):227–253.
7. Donea J. Arbitrary Lagrangian-Eulerian finite elements method. In *Computational Methods for Transient Analysis*, Belytschko T, Hughes TJR (eds): North-Holland, Amsterdam, 1983; 473–516.
8. Donea J, Huerta A. *Finite Element Methods for Flow Problems*. John Wiley and Sons, 2003.

Q3





DOI: 10.1002/fld

9. Hughes TJR, Liu WK, Zimmermann TK. Lagrangian–Eulerian finite elements formulations for incompressible viscous flows. *US-Japan Interdisciplinary Finite Element Analysis* 1978.
10. Trepanier JY, Reggio M, Zhang H, Camarero R. A finite-volume method for the Euler equations on arbitrary Lagrangian–Eulerian grids. *Computers & fluids* 1991; **20**(4):399–40.
11. Zienkiewics O, Morgan K. *Finite Element and Approximation*. John Wiley & Sons, 1983.
12. Thomas PD, Lombard CK. Geometric conservation law and its applications to flow computations on moving grids. *AIAA* 1979; **17**:1030–1037.
13. Étienne S, Garon A, Pelletier D. Perspective on the geometric conservation law and finite element methods for ALE simulations of incompressible flow. *Journal of Computational Physics* 2009; **228**(7):2313–2333.
14. Guillard H, Farhat C. On the significance of the geometric conservation law for flow computations on moving meshes. *Computer Methods in Applied Mechanics and Engineering* 2000; **190**:1467–1482.
15. Boffi D, Gastaldi L. Stability and geometric conservation laws for ALE formulations. *Computer Methods in Applied Mechanics and Engineering* 2004; **193**:4717–4739.
16. Formaggia L, Nobile F. Stability analysis of second-order time accurate schemes for ALE–FEM. *Computer Methods in Applied Mechanics and Engineering* 2004; **193**(39–41):4097–4116.
17. Geuzaine P, Grandmont C, Farhat C. Design and analysis of ALE schemes with provable second-order time-accuracy for inviscid and viscous flow simulations. *Journal of Computational Physics* 2003; **191**(1):206–227.
18. Farhat C, Geuzaine P, Grandmont C. The discrete geometric conservation law and the nonlinear stability of ALE schemes for the solution of flow problems on moving grids. *Journal of Computational Physics* 2001; **1974**:669–694.
19. Ahn HT, Kallinderis Y. Strongly coupled flow/structure interactions with a geometrically conservative ALE scheme on general hybrid meshestitle. *Journal of Computational Physics* 2006; **219**:671–693.
20. Lesoinne M, Farhat C. Geometric conservation laws for flow problems with moving boundaries and deformable meshes, and their impact on aeroelastic computations. *Computer Methods in Applied Mechanics and Engineering* 1996; **134**:71–90.
21. Mavriplis DJ, Yang Z. Achieving higher-order time accuracy for dynamic unstructured mesh fluid flow simulations: role of the GCL. *17th AIAA Computational Flow Dynamics Conference*, 2005.
22. Farhat C, Geuzaine P. Design and analysis of robust ALE time-integrators for the solution of unsteady flow problems on moving grids. *Computer Methods in Applied Mechanics and Engineering* 2004; **193**:4073–4095.
23. Nobile F. Numerical approximation of fluid-structure interaction problems with application to haemodynamics. *PhD Thesis*, École Polytechnique Fédérale de Lausanne, 2001.
24. Franca LP, Frey SL, Hughes TJR. Stabilized finite element methods: I. Application to the advective-diffusive. *Computer Methods in Applied Mechanics and Engineering* 1992; **95**:253–276.
25. Ascher U, M. *Numerical Methods for Evolutionary Differential Equations*. SIAM, 2008. Q4





DOI: 10.1002/fld

# Author Query Form

## Journal: International Journal for Numerical Methods in Fluids

## Article: fld_2669

Dear Author,

During the copyediting of your paper, the following queries arose. Please respond to these by annotating your proofs with the necessary changes/additions.

- If you intend to annotate your proof electronically, please refer to the E-annotation guidelines.
- If you intend to annotate your proof by means of hard-copy mark-up, please refer to the proof mark-up symbols guidelines. If manually writing corrections on your proof and returning it by fax, do not write too close to the edge of the paper. Please remember that illegible mark-ups may delay publication.

Whether you opt for hard-copy or electronic annotation of your proofs, we recommend that you provide additional clarification of answers to queries by entering your answers on the query sheet, in addition to the text mark-up.

| Query No. | Query | Remark |
|---|---|---|
| Q1 | AUTHOR: Figure 16 contains very small texts which are unreadable. Please resupply at 600/300 dpi. Check required artwork specifications at http://www.blackwellpublishing.com/authors/digill.asp | |
| Q2 | AUTHOR: Please provide a suitable legend for Figure A.1. | |
| Q3 | AUTHOR: Please provide publisher location for Reference 8. | |
| Q4 | AUTHOR: Please provide publisher location for Reference 25. | |

# USING E-ANNOTATION TOOLS FOR ELECTRONIC PROOF CORRECTION

## Required Software

Adobe Acrobat Professional or Acrobat Reader (version 7.0 or above) is required to e-annotate PDFs. Acrobat 8 Reader is a free download: http://www.adobe.com/products/acrobat/readstep2.html

Once you have Acrobat Reader 8 on your PC and open the proof, you will see the Commenting Toolbar (if it does not appear automatically go to Tools>Commenting>Commenting Toolbar). The Commenting Toolbar looks like this:

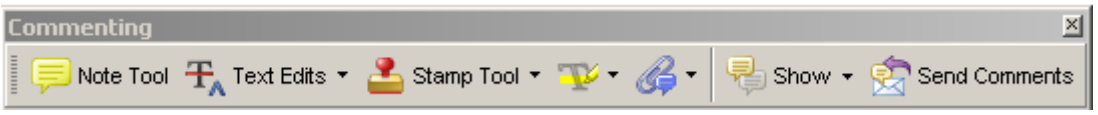


If you experience problems annotating files in Adobe Acrobat Reader 9 then you may need to change a preference setting in order to edit.

In the "Documents" category under "Edit – Preferences", please select the category 'Documents' and change the setting "PDF/A mode:" to "Never".

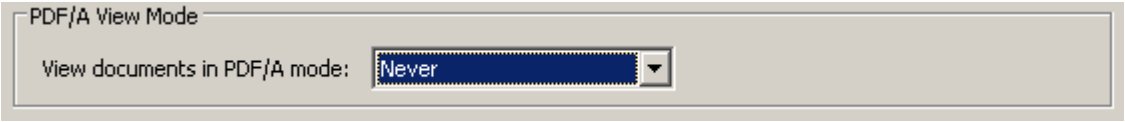


## Note Tool — For making notes at specific points in the text

Marks a point on the paper where a note or question needs to be addressed.

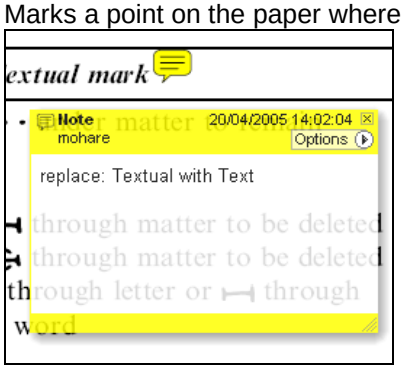


**How to use it:**

1. Right click into area of either inserted text or relevance to note
2. Select Add Note and a yellow speech bubble symbol and text box will appear
3. Type comment into the text box
4. Click the X in the top right hand corner of the note box to close.

## Replacement text tool — For deleting one word/section of text and replacing it

Strikes red line through text and opens up a replacement text box.

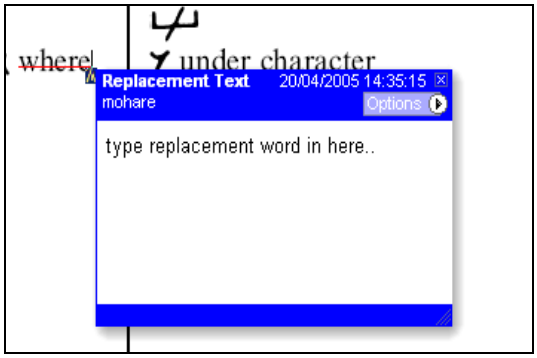


**How to use it:**

1. Select cursor from toolbar
2. Highlight word or sentence
3. Right click
4. Select Replace Text (Comment) option
5. Type replacement text in blue box
6. Click outside of the blue box to close

## Cross out text tool — For deleting text when there is nothing to replace selection

Strikes through text in a red line.

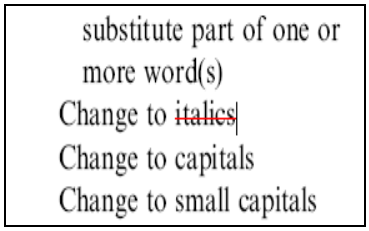


**How to use it:**

1. Select cursor from toolbar
2. Highlight word or sentence
3. Right click
4. Select Cross Out Text

## Approved tool — For approving a proof and that no corrections at all are required.


**How to use it:**

1. Click on the Stamp Tool in the toolbar
2. Select the Approved rubber stamp from the 'standard business' selection
3. Click on the text where you want to rubber stamp to appear (usually first page)

## Highlight tool — For highlighting selection that should be changed to bold or italic.

Highlights text in yellow and opens up a text box.

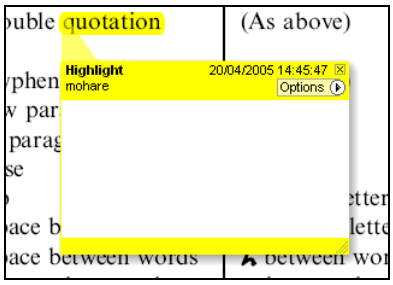


**How to use it:**

1. Select Highlighter Tool from the commenting toolbar
2. Highlight the desired text
3. Add a note detailing the required change

## Attach File Tool — For inserting large amounts of text or replacement figures as a files.

Inserts symbol and speech bubble where a file has been inserted.

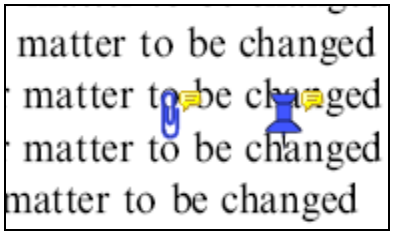


**How to use it:**

1. Click on paperclip icon in the commenting toolbar
2. Click where you want to insert the attachment
3. Select the saved file from your PC/network
4. Select appearance of icon (paperclip, graph, attachment or tag) and close

## Pencil tool — For circling parts of figures or making freeform marks

Creates freeform shapes with a pencil tool. Particularly with graphics within the proof it may be useful to use the Drawing Markups toolbar. These tools allow you to draw circles, lines and comment on these marks.

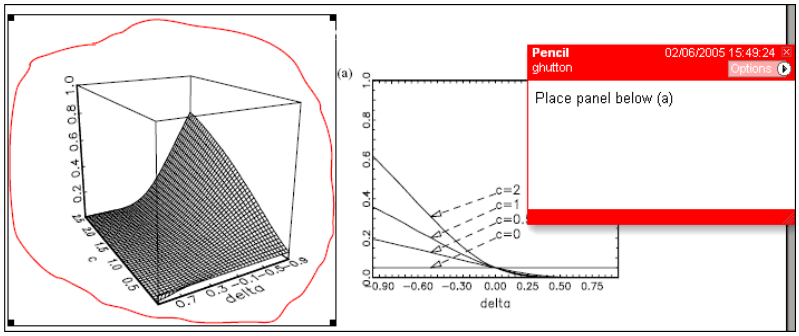


**How to use it:**

1. Select Tools > Drawing Markups > Pencil Tool
2. Draw with the cursor
3. Multiple pieces of pencil annotation can be grouped together
4. Once finished, move the cursor over the shape until an arrowhead appears and right click
5. Select Open Pop-Up Note and type in a details of required change
6. Click the X in the top right hand corner of the note box to close.

## Help

For further information on how to annotate proofs click on the Help button to activate a list of instructions:

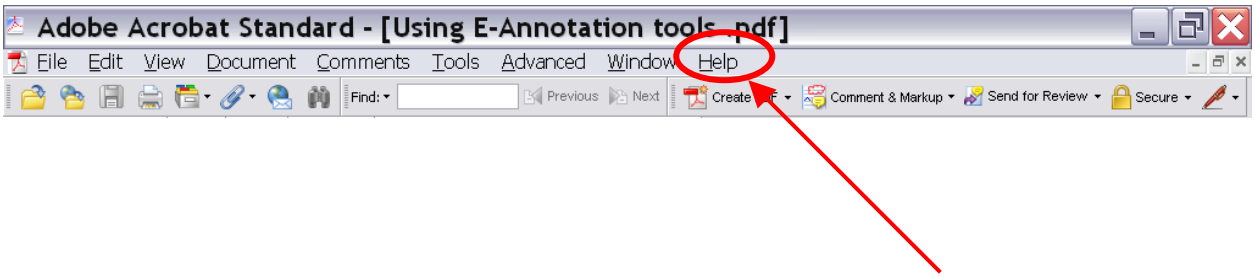

# WILEY AUTHOR DISCOUNT CLUB

We would like to show our appreciation to you, a highly valued contributor to Wiley's publications, by offering a **unique 25% discount** off the published price of any of our books*.

All you need to do is apply for the **Wiley Author Discount Card** by completing the attached form and returning it to us at the following address:

The Database Group (Author Club)
John Wiley & Sons Ltd
The Atrium
Southern Gate
Chichester
PO19 8SQ
UK

Alternatively, you can **register online** at www.wileyeurope.com/go/authordiscount
Please pass on details of this offer to any co-authors or fellow contributors.

After registering you will receive your Wiley Author Discount Card with a special promotion code, which you will need to quote whenever you order books direct from us.

The quickest way to order your books from us is via our European website at:

## http://www.wileyeurope.com

Key benefits to using the site and ordering online include:
- Real-time SECURE on-line ordering
- Easy catalogue browsing
- Dedicated Author resource centre
- Opportunity to sign up for subject-orientated e-mail alerts

Alternatively, you can order direct through Customer Services at:
cs-books@wiley.co.uk, or call +44 (0)1243 843294, fax +44 (0)1243 843303

So take advantage of this great offer and return your completed form today.

Yours sincerely,

Verity Leaver
Group Marketing Manager
author@wiley.co.uk

*TERMS AND CONDITIONS

This offer is exclusive to Wiley Authors, Editors, Contributors and Editorial Board Members in acquiring books for their personal use. There must be no resale through any channel. The offer is subject to stock availability and cannot be applied retrospectively. This entitlement cannot be used in conjunction with any other special offer. Wiley reserves the right to amend the terms of the offer at any time.

WILEY

# REGISTRATION FORM
# For Wiley Author Club Discount Card

To enjoy your 25% discount, tell us your areas of interest and you will receive relevant catalogues or leaflets from which to select your books. Please indicate your specific subject areas below.

**Accounting** [ ]
- Public [ ]
- Corporate [ ]

**Chemistry** [ ]
- Analytical [ ]
- Industrial/Safety [ ]
- Organic [ ]
- Inorganic [ ]
- Polymer [ ]
- Spectroscopy [ ]

**Encyclopedia/Reference** [ ]
- Business/Finance [ ]
- Life Sciences [ ]
- Medical Sciences [ ]
- Physical Sciences [ ]
- Technology [ ]

**Earth & Environmental Science** [ ]

**Hospitality** [ ]

**Genetics** [ ]
- Bioinformatics/ Computational Biology [ ]
- Proteomics [ ]
- Genomics [ ]
- Gene Mapping [ ]
- Clinical Genetics [ ]

**Medical Science** [ ]
- Cardiovascular [ ]
- Diabetes [ ]
- Endocrinology [ ]
- Imaging [ ]
- Obstetrics/Gynaecology [ ]
- Oncology [ ]
- Pharmacology [ ]
- Psychiatry [ ]

**Non-Profit** [ ]

**Architecture** [ ]

**Business/Management** [ ]

**Computer Science** [ ]
- Database/Data Warehouse [ ]
- Internet Business [ ]
- Networking [ ]
- Programming/Software Development [ ]
- Object Technology [ ]

**Engineering** [ ]
- Civil [ ]
- Communications Technology [ ]
- Electronic [ ]
- Environmental [ ]
- Industrial [ ]
- Mechanical [ ]

**Finance/Investing** [ ]
- Economics [ ]
- Institutional [ ]
- Personal Finance [ ]

**Life Science** [ ]

**Landscape Architecture** [ ]

**Mathematics** [ ]

**Statistics** [ ]

**Manufacturing** [ ]

**Materials Science** [ ]

**Psychology** [ ]
- Clinical [ ]
- Forensic [ ]
- Social & Personality [ ]
- Health & Sport [ ]
- Cognitive [ ]
- Organizational [ ]
- Developmental & Special Ed [ ]
- Child Welfare [ ]
- Self-Help [ ]

**Physics/Physical Science** [ ]

Please complete the next page /

WILEY

I confirm that I am (*delete where not applicable):

a **Wiley** Book Author/Editor/Contributor* of the following book(s):
ISBN:
ISBN:

a **Wiley** Journal Editor/Contributor/Editorial Board Member* of the following journal(s):

SIGNATURE: ..... Date: .....

---

**PLEASE COMPLETE THE FOLLOWING DETAILS IN BLOCK CAPITALS:**

TITLE: (e.g. Mr, Mrs, Dr) ..... FULL NAME: .....

JOB TITLE (or Occupation): .....

DEPARTMENT: .....

COMPANY/INSTITUTION: .....

ADDRESS: .....

.....

TOWN/CITY: .....

COUNTY/STATE: .....

COUNTRY: .....

POSTCODE/ZIP CODE: .....

DAYTIME TEL: .....

FAX: .....

E-MAIL: .....

---

**YOUR PERSONAL DATA**
We, John Wiley & Sons Ltd, will use the information you have provided to fulfil your request. In addition, we would like to:

1. Use your information to keep you informed by post of titles and offers of interest to you and available from us or other Wiley Group companies worldwide, and may supply your details to members of the Wiley Group for this purpose.
   [ ] Please tick the box if you do **NOT** wish to receive this information

2. Share your information with other carefully selected companies so that they may contact you by post with details of titles and offers that may be of interest to you.
   [ ] Please tick the box if you do **NOT** wish to receive this information.

**E-MAIL ALERTING SERVICE**
We also offer an alerting service to our author base via e-mail, with regular special offers and competitions. If you **DO** wish to receive these, please opt in by ticking the box [ ].

If, at any time, you wish to stop receiving information, please contact the Database Group (databasegroup@wiley.co.uk) at John Wiley & Sons Ltd, The Atrium, Southern Gate, Chichester, PO19 8SQ, UK.

---

**TERMS & CONDITIONS**
This offer is exclusive to Wiley Authors, Editors, Contributors and Editorial Board Members in acquiring books for their personal use. There should be no resale through any channel. The offer is subject to stock availability and may not be applied retrospectively. This entitlement cannot be used in conjunction with any other special offer. Wiley reserves the right to vary the terms of the offer at any time.

**PLEASE RETURN THIS FORM TO:**
Database Group (Author Club), John Wiley & Sons Ltd, The Atrium, Southern Gate, Chichester, PO19 8SQ, UK author@wiley.co.uk
Fax: +44 (0)1243 770154